Electronic Supporting Information

Selective hydrogenation of furfural on intermetallic compounds with outstanding catalytic performance

Yusen Yang,‡[a] Lifang Chen,‡[a] Yudi Chen,[b] Wei Liu,[a] Haisong Feng,[a] Bin Wang,[c] Xin Zhang,*[a] Min Wei*[a]

[a] *State Key Laboratory of Chemical Resource Engineering, Beijing Advanced Innovation Center for Soft Matter Science and Engineering, Beijing University of Chemical Technology, Beijing 100029, P. R. China*

[b] *Beijing Center for Physical & Chemical Analysis, Beijing 100089, P. R. China*

[c] *Beijing Research Institute of Chemical Industry, Sinopec Group, Beijing 100013, P. R. China*

Author Information

‡ These authors contribute equally to this work.

* Corresponding authors. Tel: +86-10-64412131; Fax: +86-10-64425385.

E-mail addresses: zhangxin@mail.buct.edu.cn (X. Zhang); weimin@mail.buct.edu.cn (M. Wei).

Table S1 Lattice parameters (Å) of bulk Ni_3Sn_2 from PBE, PW91, PBEsol, and PBE-D3 functionals

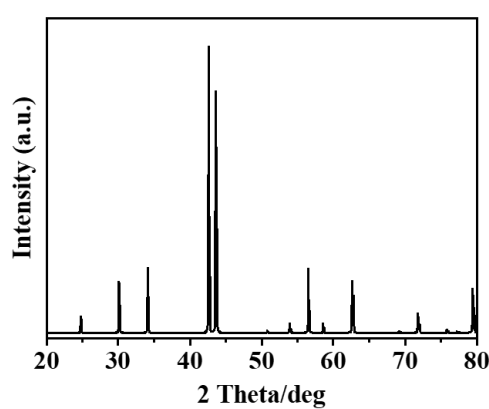| GGA functional	Lattice constant/Å			Volume deviation
	a	b	c	
PBE	4.29	4.29	5.29	0.07%
PW91	4.29	4.29	5.30	0.10%
PBEsol	4.23	4.23	5.21	0.20%
PBE-D3	4.25	4.25	5.24	0.01%
Expt.[1]	4.15	4.15	5.25	-

Fig. S1 Reflex powder diffraction pattern of Ni_3Sn_2 crystalloid simulated by computer.

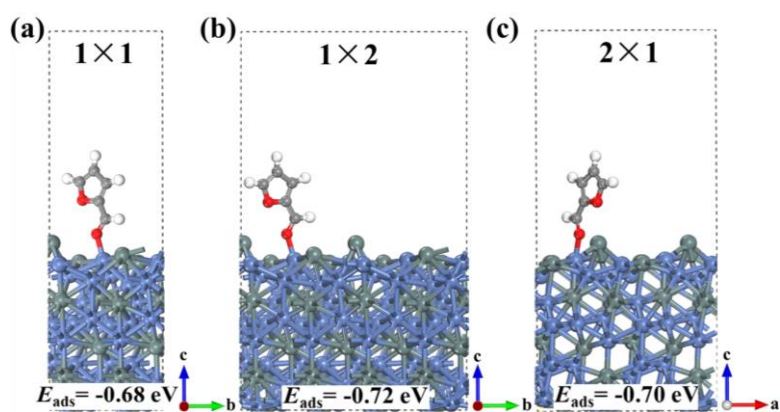**Fig. S2** Adsorption energies of furfural on the surface of $Ni_3Sn_2(101)$ with various crystal size.

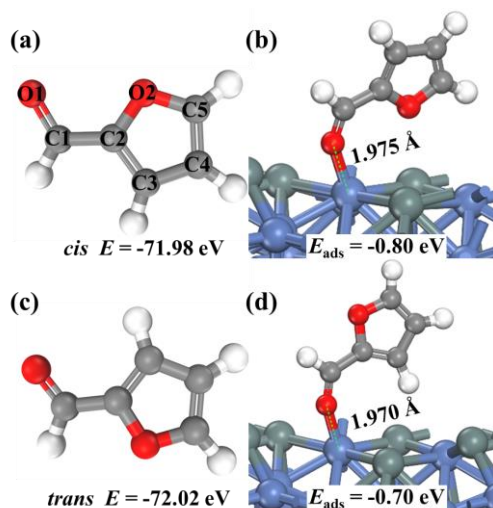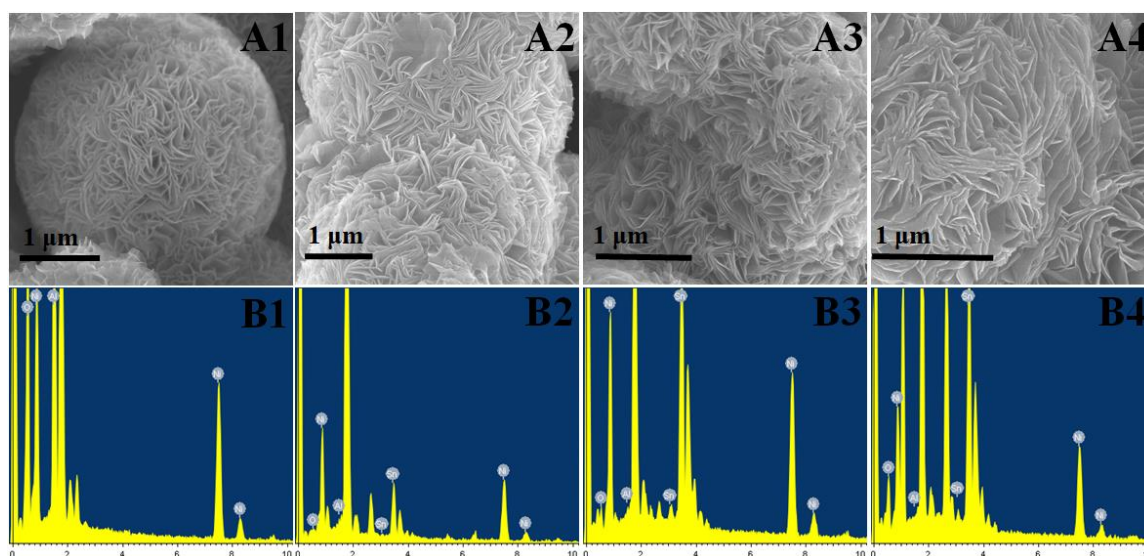**Fig. S3** Optimized adsorption structures and adsorption energies of *cis*-, *trans*-furfural on $Ni_3Sn_2(101)$.

Fig. S4 SEM images of (A1) the as-synthesized Ni_2Al-LDHs precursor and the $Sn(OH)_4/Ni_2Al$-LDHs mixtures with Sn/Ni molar ratio of (A2) 1/3, (A3) 2/3, (A4) 4/3, respectively. EDS analysis of (B1) the as-synthesized Ni_2Al-LDHs precursor and the $Sn(OH)_4/Ni_2Al$-LDHs mixtures with total Sn/Ni molar ratio of (B2) 1/3, (B3) 2/3, (B4) 4/3, respectively.
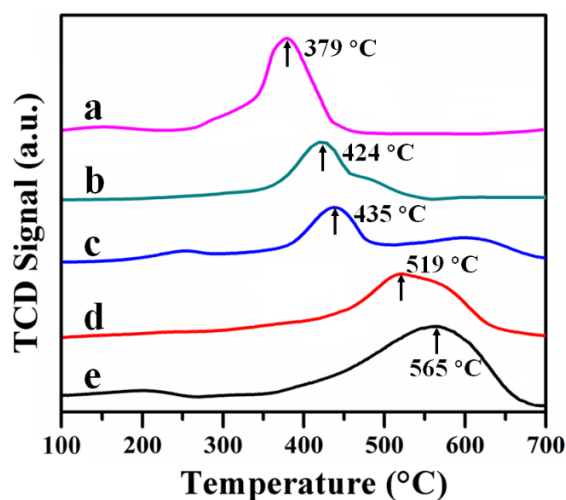
Fig. S5 H_2-TPR profiles for (a) the as-synthesized Ni_2Al-LDHs precursor, the $Sn(OH)_4/Ni_2Al$-LDHs mixtures with total Sn/Ni molar ratio of (b) 1/3, (c) 2/3, (d) 4/3, and (e) $Sn(OH)_4$, respectively.

Table S2 Bader charges analysis of pristine Ni, Ni_3Sn_1, Ni_3Sn_2 and Ni_3Sn_4

Sample	Atom	Charge
Sn	Sn	0.00
Ni	Ni	0.00
Ni_3Sn_1	Sn^a	+0.51
	$Ni1^b$	−0.18
	$Ni2^b$	−0.16
	$Ni3^b$	−0.17
Ni_3Sn_2	$Sn1^a$	+0.49
	$Sn2^a$	+0.49
	$Ni1^b$	−0.09
	$Ni2^b$	−0.09
	$Ni3^b$	−0.80
Ni_3Sn_4	$Sn1^a$	+0.26
	$Sn2^a$	+0.30
	$Sn3^a$	+0.33
	$Sn4^a$	+0.34
	$Ni1^b$	−0.44
	$Ni2^b$	−0.40
	$Ni3^b$	−0.39

[a] Different Sn atoms in Ni-Sn IMCs.

[b] Different Ni atoms in Ni-Sn IMCs.

Table S3 Curve-fitting and DFT calculation results of Ni K-edge EXAFS spectra of pristine Ni, Ni_3Sn_1, Ni_3Sn_2 and Ni_3Sn_4

Sample	Shell	R(Å) –CF[a]	R(Å) –DFT[b]	CN –CF[c]	CN –DFT[d]	$\Delta\sigma^2$(Å)[e]
Ni	Ni–Ni	2.482	2.457	11	11	0.0061
Ni_3Sn_1	Ni–Ni	2.585	2.565	5	5	0.0149
	Ni–Sn	2.630	2.617	2	2	0.0056
Ni_3Sn_2	Ni–Ni	2.622	2.645	3	3	0.0124
	Ni–Sn	2.506	2.568	5	5	0.0173
Ni_3Sn_4	Ni–Ni	2.661	2.703	1	1	0.0060
	Ni–Sn	2.613	2.632	7	7	0.0080

[a] Distance between absorber and backscatter atom, determined by curve fitting.

[b] Distance between absorber and backscatter atom, determined by DFT calculation.

[c] Coordination number, determined by curve fitting.

[d] Coordination number, determined by DFT calculation.

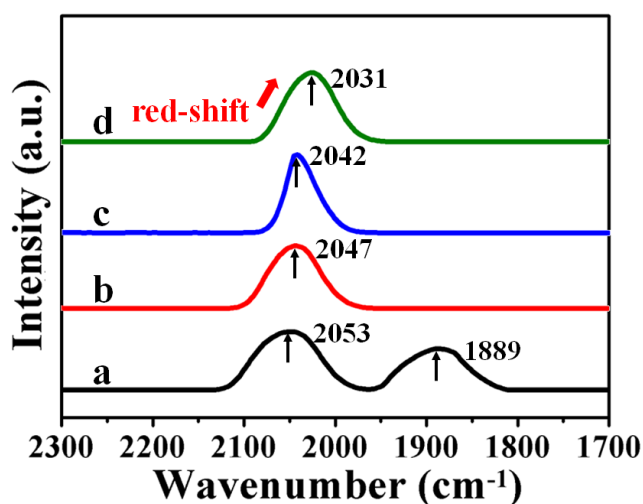[e] Change in the Debye-Waller factor value relative to the reference sample.

Fig. S6 *In situ* Fourier-transformed infrared spectra of CO adsorption over (a) Ni, (b) Ni_3Sn_1, (c) Ni_3Sn_2, and (d) Ni_3Sn_4, respectively.
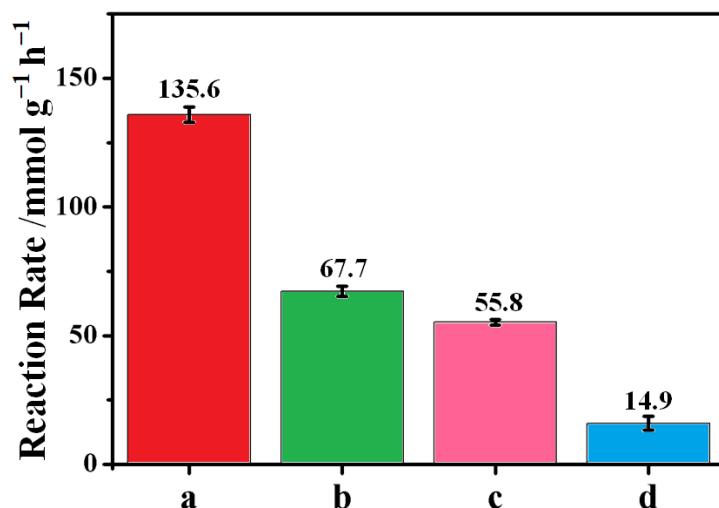
Fig. S7 Reaction rate for furfural hydrogenation over (a) Ni, (b) Ni_3Sn_1, (c) Ni_3Sn_2, and (d) Ni_3Sn_4, respectively. Reaction rate is calculated on the basis of tangent slope of the conversion-reaction time plot within 20−40% conversion of furfural.
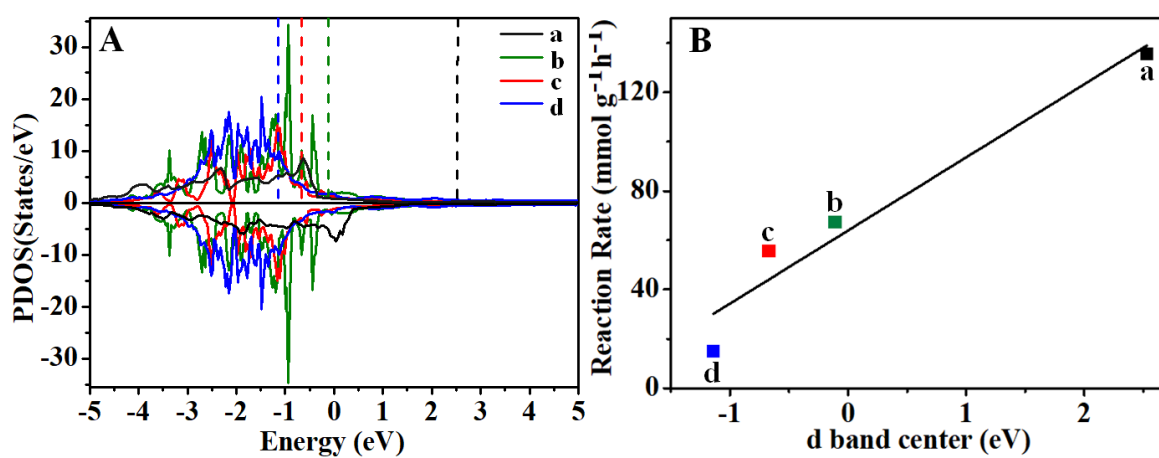

Fig. S8 (A) Projected density of states of Ni-3d state in: (a) Ni, (b) Ni_3Sn_1, (c) Ni_3Sn_2, (d) Ni_3Sn_4. Corresponding dash lines represent the *d* band center for the bulk Ni (2.53 eV), Ni_3Sn_1 (−0.11 eV), Ni_3Sn_2 (−0.67 eV) and Ni_3Sn_4 (−1.14 eV). (B) Reaction rate *vs. d* band center of (a) Ni, (b) Ni_3Sn_1, (c) Ni_3Sn_2, (d) Ni_3Sn_4.

Table S4 Comparison of catalytic performance for selective hydrogenation of furfural to furfuryl alcohol over various catalysts
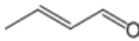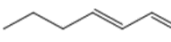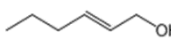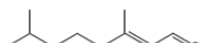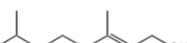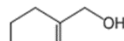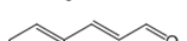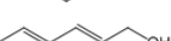
Entry	Catalyst	Time (h)	Conversion (%)	Selectivity (%)	Reaction Rate (mmol g^{-1} h^{-1})	Ref.
1	Ni/Al$_2$O$_3$	3	100	2	135.6	This work
2	Ni$_3$Sn$_1$/Al$_2$O$_3$	3	100	75	67.7	This work
3	Ni$_3$Sn$_2$/Al$_2$O$_3$	3	100	99	55.8	This work
4	Ni$_3$Sn$_4$/Al$_2$O$_3$	3	38	99	14.9	This work
5	Ni/C	3	67	60	52.6	[2]
6	Ni/SiO$_2$	3	99	50	46.9	[2]
7	Ni-Cu/TiO$_2$	2	91	35	62.8	[3]
8	Ni-Cu/Al$_2$O$_3$	2	99	3	65.2	[3]
9	Ni-Fe(2)HT-673	3	99	96	43.1	[4]
10	Ni-Co(1)HT-673	3	85	89	38.5	[4]
11	20NiCoB/SiO$_2$	2	54	83	26.3	[5]
12	20NiCoB/ Al$_2$O$_3$	2	52	91	24.1	[5]
13	Pt@mSiO$_2$	5	25	34	11.4	[6]
14	PtSn@mSiO$_2$	5	99	97	49.8	[6]
15	Pt/Al$_2$O$_3$	7	80	99	30.1	[7]
16	Pt/MgO	7	79	97	29.7	[7]
17	Pt/CeO$_2$NH$_2$	7	77	98	28.4	[7]
18	Pt-CeO$_2$@UIO	1	100	98	78.3	[8]
19	Pt-CeO$_2$	1	99	1	77.4	[8]

Table S5 Catalytic performance of Ni_3Sn_2 after storage in air for one week

Entry	Catalyst	Exposure Atmosphere	Exposure Time	Conversion (%)	Selectivity (%)
1	Ni_3Sn_2/Al_2O_3	--	--	100	99
2	Ni_3Sn_2/Al_2O_3	Air	1 day	100	98
3	Ni_3Sn_2/Al_2O_3	Air	3 days	97	97
4	Ni_3Sn_2/Al_2O_3	Air	5 days	95	96
5	Ni_3Sn_2/Al_2O_3	Air	7 days	95	96

Reaction conditions: furfural/Ni = 58 (molar ratio); furfural, 1.0 mL; iso-PrOH, 30 mL; temperature, 100 °C; H_2 pressure, 2 MPa; reaction time, 4 h.

Table S6 Catalytic performance for hydrogenation of different kinds of unsaturated aldehydes over Ni and Ni_3Sn_2 IMC

Entry	Substrate	Product	Ni		Ni_3Sn_2	
			Con.	Sel.	Con.	Sel.
1			91%	0	45%	54%
2			100%	1%	42%	71%
3			97%	0	64%	62%
4			76%	2%	23%	69%
5			80%	1%	36%	57%
6			92%	1%	49%	32%

Reaction conditions: furfural/Ni = 58 (molar ratio); furfural, 1.0 mL; iso-PrOH, 30 mL; temperature, 100 °C; H_2 pressure, 2 MPa, reaction time, 6 h.
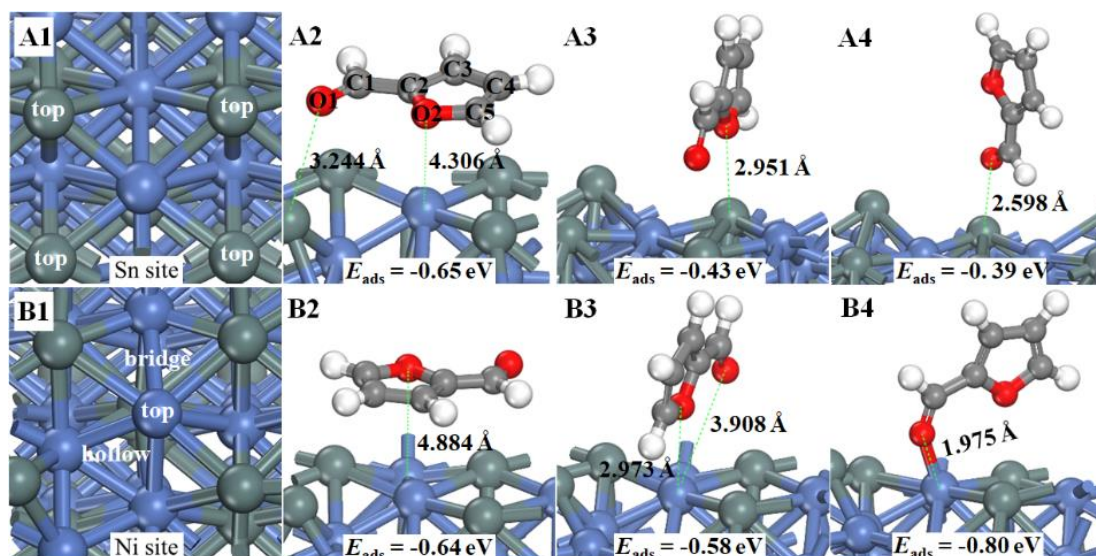
Fig. S9 Optimized adsorption structures and adsorption energies of furfural at Sn site (A1−A4) and Ni site (B1−B4) on the surface of Ni$_3$Sn$_2$(101).

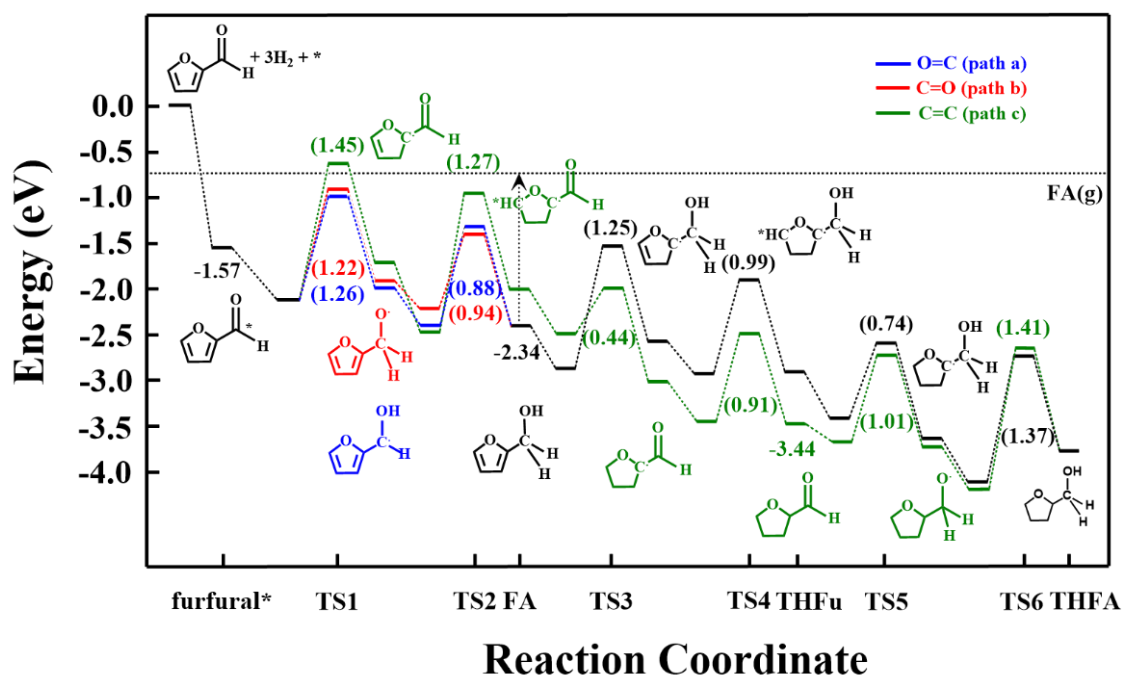**Fig. S10** Potential energy profiles for hydrogenation of furfural to tetrahydrofurfuryl alcohol on Ni(111) surface. Red line, H atom attacks O1. Blue lines, H atom attacks C1. Green line, H atom attacks C3 in furfural. The black arrow represents desorption of furfuryl alcohol. Numbers in the parentheses represent reaction barriers of elementary step, and others stands for adsorption energies.

Table S7 Free energies at various reaction temperatures involved in the reaction process (R1−R5)

Free energies/eV	R1	R2	R3	R4	R5
ΔG(353 K)	−0.60	−0.47	0.23	0.82	0.52
ΔG(363 K)	−0.60	−0.47	0.23	0.83	0.51
ΔG(373 K)	−0.59	−0.46	0.24	0.84	0.50
ΔG(383 K)	−0.59	−0.45	0.24	0.85	0.40
ΔG(393 K)	−0.58	−0.44	0.24	0.87	0.49

Table S8 Equilibrium constant for step R1−R3 and reaction rate constant for Step R3 and R4 at various reaction temperatures

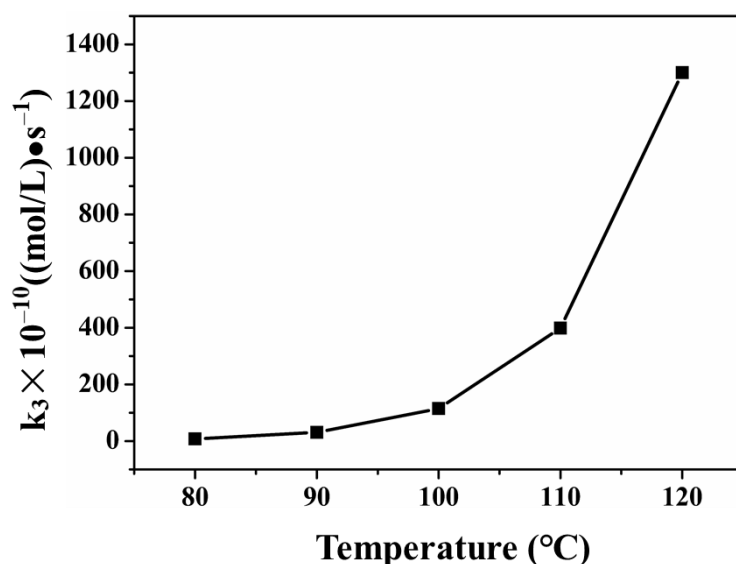| T/K	K_1 (mol/L)$^{-1}$	K_2 (mol/L)$^{-1}$	K_3	k_3 (mol/L)·s^{-1}	k_4 (mol/L)·s^{-1}
353	4.22×10^8	5.64×10^6	4.76×10^{-4}	7.71×10^{-10}	186.47
363	2.05×10^8	2.91×10^6	5.52×10^{-4}	3.09×10^{-9}	331.07
373	1.03×10^8	1.56×10^6	6.35×10^{-4}	1.15×10^{-8}	569.91
383	5.38×10^7	8.61×10^5	7.25×10^{-4}	3.99×10^{-8}	683.31
393	2.91×10^7	4.91×10^5	8.21×10^{-4}	1.30×10^{-7}	765.06

Fig. S11 Rate constant k_3 as a function of reaction temperature.

References

[1] H. Fjellvåg, A. Kjekshus, *Acta Chem. Scand., A* 1986, **40**, 23−30.

[2] H. Jeong, C. Kim, S. Yang, H. Lee, *J. Catal.*, 2016, **344**, 609−615.

[3] B. Seemala, C. M. Cai, C. E. Wyman, P. Christopher, *ACS Catal.*, 2017, **7**, 4070−4082.

[4] W. S. Putro, T. Kojima, T. Hara, N. Ichikuni, S. Shimazu, *Catal. Sci. Technol*. 2017, **7**, 3637–3646.

[5] H. Guo, H. Zhang, L. Zhang, C. Wang, F. Peng, Q. Huang, L. Xiong, C. Huang, X. Ouyang, X. Chen, X. Qiu, *Ind. Eng. Chem. Res.,* 2018, **57**, 498−511.

[6] R. V. Maligal-Ganesh, C. Xiao, T. W. Goh, L. Wang, J. Gustafson, Y. Pei, Z. Qi, D. D. Johnson, S. Zhang, F. Tao, W. Huang, *ACS Catal.,* 2016, **6**, 1754−1763.

[7] M. J. Taylor, L. J. Durndell, M. A. Isaacs, C. M. A. Parlett, K. Wilson, A. F. Lee, G. Kyriakou, *Appl. Catal., B Environ.,* 2016, **180**, 580−585.

[8] Y. Long, S. Song, J. Li, L. Wu, Q. Wang, Y. Liu, R. Jin, H. Zhang, *ACS Catal.,* 2018, **8**, 8506−8512.